Processing weak electrical signals with threshold-potential nanostructures showing a high variability

José A. Manzanares, Javier Cervera, and Salvador Mafé[a)]
Facultat de Física, Universitat de València, E-46100 Burjassot, Spain

(Received 21 June 2011; accepted 20 September 2011; published online 12 October 2011)

We explore the processing of weak electrical signals in parallel arrays of bio-inspired threshold nanostructures showing a high variability in their threshold potentials. We consider a two-state canonical model that incorporates the basic properties demonstrated experimentally. The model is inspired by the voltage-gated ion channels in biological membranes and shows that the nanostructure variability can allow significant transmission of sub-threshold signals. Implications for the design of practical devices are briefly discussed. © *2011 American Institute of Physics*. [doi:10.1063/1.3650712]

Biological networks composed of non-identical threshold nanostructures can process weak electrical signals in a noisy environment. This is the case of clusters of ion channels in biological membranes and neuronal sensory networks in the brain, where the variability between the effective threshold potentials of the processing units arises from the intrinsic biological diversity, the complexity of local connections, and the possibility of conductance modulation by different species in solution.[1–6] Remarkably, when trying to design bio-inspired devices on the basis of functionalized nanopores and nanoparticles,[7,8] the fabrication uncertainties may result also in a high variability in the threshold potentials.[9,10]

The implementation of logical and signal processing schemes using nanostructures is expected to have a low reliability because of the weak signals involved, the thermal noise, and the high individual variability in the threshold potentials. The biochemical diversity of the ion channels inserted in lipid bilayers,[3–6,11] the different pore shapes and surface functionalizations of synthetic nanopores,[7,8] and the size distribution of nanoparticles[8–10] and nanowires[12] result in a significant spread of their individual threshold potentials. The threshold voltage mismatching of electronic transistors can also have profound effects in voltage-driven applications.[13]

We explore theoretically the signal processing in parallel arrays of bio-inspired nanostructures showing a high variability in their threshold potentials. The diversity-induced *static* noise that originates from the *hardware* variability is considered together with the *dynamic* noise of the input signal. The simulations suggest that in some cases moderate redundancy permits to minimize the adverse effects of the hardware diversity and to exploit the threshold fluctuations in order to increase the detection range of weak signals. The basic concepts involved are commonplace in biophysics[3–5,11] and should be of interest for the design of reliable information processing schemes with non-identical nanostructures. Potential applications include processing of weak signals with biological channels inserted in lipid bilayers,[4,11] synthetic nanopores,[7,8] arrays of functionalized nanoparticles,[8,9] nanowire field-effect transistors,[12] and nanoswitches based on molecular dipoles.[14,15]

We make use of a simple model that incorporates the effect of the bistable nature of the nanostructure on the charge transport dynamics. The model is inspired by the voltage-gated ion channels of biological membranes,[1–6] incorporates some of the basic properties demonstrated experimentally, and is amenable to fundamental analysis. When the applied potential is V, the probability $p(V|V_{\mathrm{th},i})$ of finding a nanostructure i of threshold potential $V_{\mathrm{th},i}$ in the high conductance state is given by the canonical distribution

$$\frac{p(V|V_{\mathrm{th},i})}{1-p(V|V_{\mathrm{th},i})} = \exp[ze(V-V_{\mathrm{th},i})/kT], \tag{1}$$

where k is Boltzmann's constant, T is the absolute temperature, and e is the elementary charge. Thus, charge transport is significant when $V > V_{\mathrm{th},i}$. The parameter z quantifies the sensitivity of the system to the potential inputs in the vicinity of the transition region between two states of high and low conductance. For ion channels, the threshold potential is related to the energy barrier due to the conformational changes needed to open the channel, and z is the equivalent gating charge number. This parameter depends on the number of charges moving across a fraction of the total potential applied through the channel.[3]

Figure 1(a) shows a typical current-voltage curve for a model nanostructure with two regions of low (g) and high conductance (G) separated by a non-linear transition region around the threshold potential. This behavior is a characteristic of both biological[2,3] and artificial[12,15,16] threshold systems. We will assume that $G \gg g \approx 0$ and analyze the processing of an input signal $V(t)$ using a parallel array of N non-identical nanostructures. Current experimental procedures produce nanostructures with a high variability in their properties, and this leads to statistical distributions of probability $p(V_{\mathrm{th},i})$ for the values $V_{\mathrm{th},i}$ of the individual threshold potentials. Thus, each nanostructure has a different current under the same applied potential V (those nanostructures with $V_{\mathrm{th},i} > V$ show a small current). The average current per nanostructure is

a)Author to whom correspondence should be addressed. Electronic mail: smafe@uv.es.

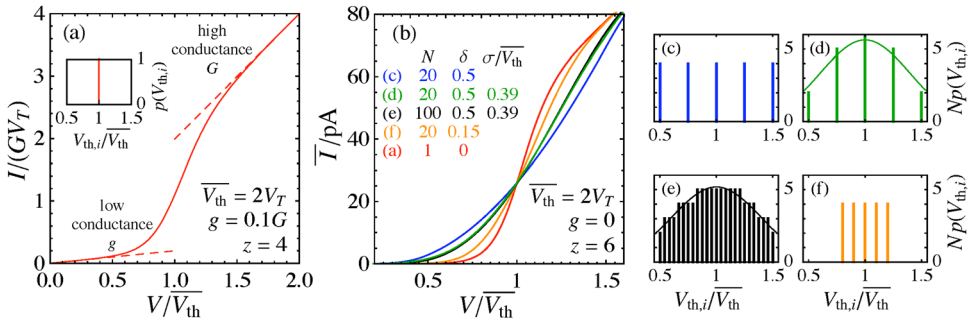

FIG. 1. (Color online) (a) Steady-state I-V curve of a nanostructure. The low and high conductance regimes are separated by a non-linear transition region around the threshold voltage $\bar{V}_{th}$. $V_T = kT/e$ is the thermal electric potential. (b) Average current per nanostructure vs. $V/\bar{V}_{th}$ for a parallel array of N nanostructures whose distribution of threshold potentials has mean $\bar{V}_{th}$, relative variability δ, and standard deviation σ. The distributions considered are shown in (a) and (c)-(f) and their parameters are given in (b). The parameter values used are $G = 1$ nS, $z = 6$, and $\bar{V}_{th} = 2V_T$ (=52 mV at 300 K).

$$\bar{I}(t) = GV(t)\frac{1}{N}\sum_{i=1}^{N} p(V(t)|V_{th,i}) = GV(t)\sum_{V_{th,i}} p(V_{th,i})p(V(t)|V_{th,i}), \quad (2)$$

where $Np(V_{th,i})$ is the number of nanostructures with threshold potential $V_{th,i}$. We have considered discretized and truncated Gaussian distributions of $N/4$ different threshold potentials $V_{th,i}$, with mean $\bar{V}_{th}$ and standard deviation σ, spanning the range $1-\delta \le V_{th,i}/\bar{V}_{th} \le 1+\delta$, where δ is the relative variability. Examples are given in Figs. 1(a) and 1(c)–1(f). The individual threshold potentials $V_{th,i}$ vary from 26 to 78 mV when $\delta = 0.5$ and $\bar{V}_{th} = 52$ mV.

Equations (1) and (2) show some of the essential characteristics of threshold systems. We present simulations with different probability distributions to study the effect of variability on the correlation between the *input* potential and the *output* current. The absolute value of the current and its fluctuations are analyzed as a function of the number of nanostructures, applied potential, and nanostructure individual characteristics in Figs. 1–3. We assume that the time variation of $V(t)$ is slow enough for the system to follow instantaneously the external perturbation. This assumption is reasonable for nanostructures characterized by relatively fast time responses and, in particular, for the case of ion channels and nanopores because of the small solution volumes involved.[4,7,17] The processing of weak, *sub-threshold* input signals $V(t) < \bar{V}_{th}$ is of interest because the threshold variability results then in an increased total current with respect to the case $\delta = 0$. The nanostructures with smaller threshold potentials show much higher currents than those with larger threshold potentials because of the upward concavity of the I-V curve in the sub-threshold regime (see Fig. 1(b)).

Figure 2 shows the average current per nanostructure $\bar{I}(t)$ when the sub-threshold multi-step potential $V(t) = V_0[H(t) + H(t-\tau) + H(t-2\tau) + H(t-3\tau)]$ is applied to a parallel array with $N = 20$, $\delta = 0.5$, and $\sigma = 0.39\bar{V}_{th}$ (higher currents). Here, $H(t)$ is the Heaviside step function, τ is the time of each potential step and $V_0 = 0.2\bar{V}_{th}$. A Gaussian white noise (GWN) of zero mean and standard deviation $0.05V_T$ has been added to the input potential. This potential has been scaled to the average threshold potential $\bar{V}_{th} = 2V_T = 52$ mV, and the distribution of threshold potentials is shown in Fig. 2(b). The current for identical nanostructures ($\delta = 0$, lower currents) has also been shown for comparison. The effect of variability becomes more marked when the sensitivity parameter z is increased (see Figs. 2(c) and 2(d)). The current for the identical nanostructures decreases with increasing z when $V(t) < \bar{V}_{th}$, but this effect does not occur with non-identical nanostructures because of the averaging. Note also the correlation between the input and output signals for $\delta = 0.5$, even when V_0 is only $0.2\bar{V}_{th}$ and the minimum threshold potential is $V_{th,i} = 26\,\text{mV} > V_0 \approx 10\,\text{mV}$.

The relatively high current through nanostructures with low threshold potentials compensates for the low current through those nanostructures with high threshold potentials. Thus, the variability enhances the correlation between the input potential and the output current. This fact has recently been demonstrated experimentally for field-effect nanowire transistors with different individual characteristics.[12] The experimental variability resulted in a distribution of threshold potentials for the nanowires. The theoretical results of Fig. 2(d) agree qualitatively with the experimental results of Fig. 4 in Ref. 12, thus confirming that variability can be beneficial for signal processing.

The above results are not restricted to the multi-step potential. Figure 3(a) shows the average current $\bar{I}(t)$ for a sub-threshold sinusoidal input potential $V(t) = V_0\sin(2\pi t/\tau)$ with amplitude $V_0 = 0.6\bar{V}_{th}$. A GWN of zero mean and standard deviation $0.05V_T$ has been added to the input

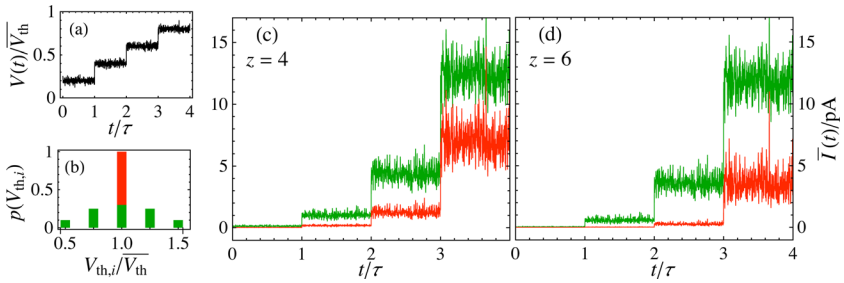

FIG. 2. (Color online) A sub-threshold multi-step potential (a) with a GWN of amplitude $0.05V_T$ is applied to 20 identical ($\delta = 0$, lower currents) and different ($\delta = 0.5$ and $\sigma = 0.39\,\bar{V}_{th}$, higher currents) nanostructures with the threshold potential distribution shown in (b). The average current per nanostructure is shown for $z = 4$ (c) and 6 (d).

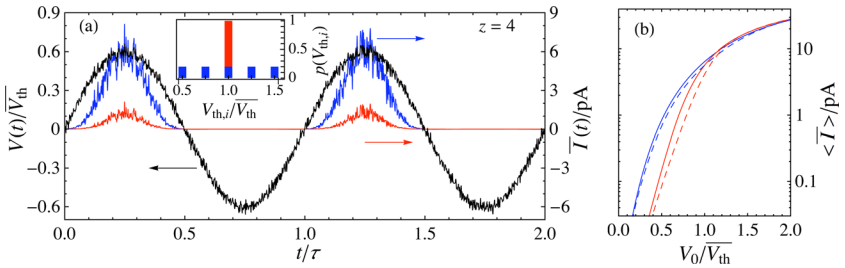

FIG. 3. (Color online) (a) Average current per nanostructure $\bar{I}(t)$ for 20 identical ($\delta = 0$, lower current) and different ($\delta = 0.5$, higher current, flat distribution) nanostructures when a sinusoidal potential of amplitude $V_0 = 0.6\ \bar{V}_{th}$ with a superimposed GWN of standard deviation $0.05V_T$ is applied. The array behaves as a half-wave rectifier because a (positive) potential close to $V_{th,i}$ is required for the nanostructure i to be in a high conductance state. In the calculations, $g = 0$, $G = 1$ nS, $z = 4$, and $\bar{V}_{th} = 2V_T$. (b) The time average current $\langle \bar{I} \rangle$ is high, in spite of the zero time average potential, because of the rectifying behavior of the array. The solid curves correspond to a sinusoidal potential with a GWN of standard deviation $0.4V_T$. The dashed curves correspond to the same potential without noise.

sinusoidal signal. The correlation between the input and output signals is higher for $\delta = 0.5$ than for $\delta = 0$. The current through nanostructure i increases *non-linearly* with V when $V < V_{th,i}$ (see Fig. 1(a)), and the contribution to the current of a fraction of nanostructures with $V_{th,i} < \bar{V}_{th}$ can be large enough to compensate for the fraction of nanostructures with $V_{th,i} > \bar{V}_{th}$. For sub-threshold signals, the time average currents $\langle \bar{I} \rangle$ obtained over a period τ are much higher for $\delta = 0.5$ than for $\delta = 0$. The presence of GWN does not change qualitatively this result.

Figure 3(b) shows that the nanostructure variability should also be of relevance for estimating the signal averaging effects caused by weak electric fields on biological cells.[17] Clusters of ion channels with different threshold potentials coexist in cell membranes, and the external fields may produce irreversible changes in the channel charge distributions. Thus, transmission of weak electrical signals across the membrane could not be completely discarded for long times because net currents might flow through the leaky patches formed by the fraction of low threshold channels.

In conclusion, biological diversity plays a role in the processing of electrical signals by non-identical threshold units,[1–6,18] and it is of interest to explore if the variability effects associated with artificial nanostructures could also be exploited in practical designs. Using a canonical model useful for different threshold systems, we have clearly shown that the variability inherent to the nanoscale can enhance significantly the processing of sub-threshold weak signals with respect to the case of identical threshold units. Cooperative effects between non-identical units[14,15] could further enhance this effect. Implications for oscillating weak electrical fields across cell membranes are also noted.

Financial support from the Ministry of Science and Innovation of Spain (Project No. MAT2009-07747) is acknowledged.

[1]R. B. Stein, E. R. Gossen, and K. E. Jones, Nat. Rev. Neurosci. **6**, 389 (2005).
[2]J. A. White, J. T. Rubinstein, and A. R. Kay, Trends Neurosci. **23**, 131 (2000).
[3]B. Hille, *Ion Channels of Excitable Membranes* (Sinauer, Sunderland, 2001).
[4]S. M. Bezrukov and I. Vodyanoy, Biophys. J. **73**, 2456 (1997).
[5]M. J. Barber and M. L. Ristig, Phys. Rev. E **74**, 041913 (2006).
[6]J. T. Rubinstein, Biophys. J. **68**, 779 (1995).
[7]M. Ali, P. Ramirez, S. Mafé, R. Neumann, and W. Ensinger, ACS Nano **3**, 603 (2009).
[8]R. W. Murray, Chem. Rev. **108**, 2688 (2008).
[9]J. Cervera, J. A. Manzanares, and S. Mafé, Nanoscale **2**, 1033 (2010).
[10]J. Cervera, J. A. Manzanares, and S. Mafé, Nanotechnology **20**, 465202 (2009).
[11]A. Alcaraz, P. Ramirez, E. Garcia-Gimenez, M. L. López, A. Andrio, and V. M. Aguilella, J. Phys. Chem. B **110**, 21205 (2006).
[12]S. Kasai, K. Miura, and Y. Shiratori, Appl. Phys. Lett. **96**, 194102 (2010).
[13]J. Pineda de Gyvez and H. P. Tuinhout, IEEE J. Solid-State Circuits **39**, 157 (2004).
[14]S. Mafé, J. A. Manzanares, and H. Reiss, J. Appl. Phys. **109**, 044302 (2011).
[15]J. A. Manzanares, J. Cervera, and S. Mafé, J. Phys. Chem. C **115**, 6980 (2011).
[16]Z. S. Siwy and S. Howorka, Chem. Soc. Rev. **39**, 1115 (2010).
[17]R. D. Astumian, J. C. Weaver, and R. K. Adair, Proc. Natl. Acad. Sci. U.S.A. **92**, 3740 (1995).
[18]H. S. Chen, J. Q. Zhang, and J. Q. Liu, Phys. Rev. E **75**, 041910 (2007).